Equation of state of hot polarized nuclear matter and heavy-ion fusion reactions

O. N. Ghodsi* and R. Gharaei
Sciences Faculty, Department of Physics, University of Mazandaran P. O. Box 47415-416, Babolsar, Iran
(Received 31 October 2010; revised manuscript received 19 June 2011; published 22 August 2011)

We employ the equation of state of hot polarized nuclear matter to simulate the repulsive force caused by the incompressibility effects of nuclear matter in the fusion reactions of heavy colliding ions. The results of our studies reveal that temperature effects of compound nuclei have significant importance in simulating the repulsive force on the fusion reactions for which the temperature of the compound nucleus increases up to about 2 MeV. Since the equation of state of hot nuclear matter depends upon the density and temperature of the nuclear matter, it has been suggested that, by using this equation of state, one can simulate simultaneously both the effects of the precompound nucleons' emission and the incompressibility of nuclear matter to calculate the nuclear potential in fusion reactions within a static formalism such as the double-folding (DF) model.

DOI: 10.1103/PhysRevC.84.024612 PACS number(s): 25.70.Jj, 21.65.Mn, 24.70.+s

I. INTRODUCTION

An appealing topic in nuclear physics is the equation state of nuclear matter which has many remarkable applications in the fusion process, the interaction of heavy ions, and astrophysics. Recent investigations of heavy-ion interactions have shown that the effects of nuclear-matter incompressibility lead to an additional repulsive force during the fusion process [1]. In the calculation of nuclear potential via the double-folding model this additional repulsive force can be simulated by adding a zero-range force to the nucleon-nucleon (NN) interaction of the M3Y type [1–3]. It has also been shown that this modification can explain the steep-fall effect in the fusion reaction [4–9]. Furthermore, our recent investigations using a BDM3Y nucleon-nucleon interaction has revealed that these modifications alter the width and height of the fusion barrier and therefore affect the calculation of the fusion cross section even in places where the energy range is higher than the height of the fusion barrier [10].

The constant parameters of this repulsive force are commonly calculated by using the Thomas-Fermi equation of state (EOS) for cold nuclear matter [11]. Considering the Q value and the energy of the incident nucleus in some of fusion reactions, the temperature of the compound nuclei produced can increase up to about 2 MeV (see, for example, Table IV). Since the nucleus loses its layered structure at temperatures above 2 MeV, it would be difficult to obtain an equation of state for the nucleus at these energies. Therefore, we have employed the equation of state of hot polarized nuclear matter (HPNM) to obtain the constant parameters of this repulsive force. In fact, the compound nucleus is assumed to be a finite piece of nuclear matter. The use of a hot equation of state is not new. This has been used in G-matrix calculations where the Pauli operator was extended for a hot G matrix, and it was used for collective flow and multifragmentation [12,13]. The entropy production and thermalization in medium-energy heavy-ion collisions was also discussed in Ref. [14].

In dynamical formalisms, contrary to a static formalism such as the DF model, one does not need to simulate the effect of nuclear-matter incompressibility by an additional NN force in the calculation of internuclear potential. This contradiction may arise from the sudden approximation that is not being used in the dynamical approaches. The other reason could be due the type of the NN forces. In the dynamical formalisms one usually uses the density-dependent NN force such as the Skyrme force to calculate the internuclear potential. In general, one of the main advantages of the dynamical formalism over the static one is that it is possible to simultaneously employ the modifying effects due to the nuclear-matter incompressibility and the escape of the nucleons during the fusion process in the calculation of the nuclear potential and fusion cross sections. Therefore, our next aim in this work is to present a mechanism within the framework of the static formalisms such as the DF model to simultaneously incorporate both of these modifications in the calculation of internuclear potential.

In Sec. II we discuss the following concepts: The EOS of HPNM, the model employed in calculating the ion-ion potential, and, finally, the effect of the nucleus temperature produced in the heavy-ion reaction on the study of the constants of additional repulsive force due to the effects of nuclear-matter incompressibility. Section IV is devoted to some concluding remarks.

II. CALCULATIONS

In nuclear fusion processes, when two nuclei completely overlap, the nuclear-matter density is twice that of the saturation density, $\rho \approx 2\rho_0$ (see Fig. 1). According to the nuclear equation of state, where the energy per nucleon is proportional to density, increasing the density in the overlap region of two interaction nuclei leads to an increase ΔU in the energy of the compound system,

$$\Delta U \approx 2A_P[E(2\rho_o) - E(\rho_o)], \tag{1}$$

where A_P is the mass number of the projectile nucleus, $E(\rho_o)$ is the energy per nucleon, and ρ_o is the saturation density of nuclear matter and is about 0.16 fm^{-3}. In most studies the equation state of cold nuclear matter has been used in the calculation of $E(\rho)$. In this paper we are going to calculate the variation of the energy, ΔU, due to the density

*o.nghodsi@umz.ac.ir

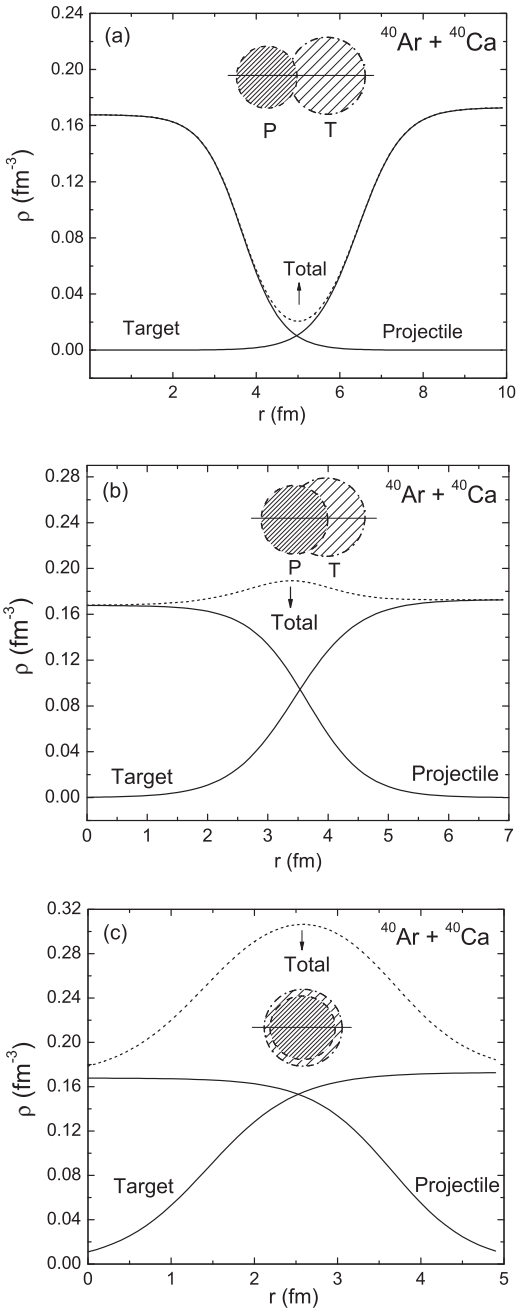

FIG. 1. Process of density-distribution overlap of the interaction nuclei for the ^{40}Ar + ^{40}Ca reaction in (a) $\rho \approx \rho_0$, (b) $\rho_0 < \rho < 2\rho_0$, and (c) $\rho \approx 2\rho_0$, where ρ and ρ_0 are density in the overlapping region and the saturation density, respectively. The total density distribution is shown by the dotted curve.

overlap of the two interacting systems, taking into account the effect of the temperature variation of the compound nucleus. As noticed earlier, the process of increasing density in the complete overlap of two nuclei is accompanied by an increase in the energy and, consequently, in the temperature of the compound nucleus. It is rather difficult to find an exact nuclear equation of state for the nuclei when the energy of the nuclei exceeds the Fermi energy so, in order to calculate the energy per nucleon of the two fully overlapped nuclei, we have used the HPNM equation of state with the approximation that the compound nucleus is taken to be as a part of nuclear matter. We have calculated the variation of energy, ΔU, by using

$$\Delta U \approx 2A_P[E_{\mathrm{HPNM}}(2\rho_o, T) - E_{\mathrm{CNM}}(\rho_o)], \tag{2}$$

where $E_{\mathrm{CNM}}(\rho_o)$ is energy per nucleon of cold nuclear matter before the interaction nuclei overlap. In order to calculate this energy we have used the Thomas-Fermi model [11,15]. $E_{\mathrm{HPNM}}(2\rho_0, T)$ is the energy per nucleon of HPNM when the two nuclei complete overlap: $\rho \approx 2\rho_0$ (see Fig. 1). This energy is considered as a function of temperature of the compound nucleus. On the other hand, in order to calculate the temperature of the compound nucleus in Eq. (2) as a function of the center-of-mass energy of the projectile nucleus, $E_{\mathrm{c.m.}}$, the following relation has been used:

$$E^* = E_{\mathrm{c.m.}} + Q_{\mathrm{in}} = \frac{1}{a}AT^2 - T, \tag{3}$$

where E^*, A, and T (in MeV) are the excitation energy, mass number, and temperature of compound nucleus, respectively. Q_{in} is the entrance-channel Q value and $a = 9$ or 10 for intermediate mass or superheavy systems, respectively. In the following subsections, we will discuss the HPNM equation of state and how to calculate internuclear potential.

A. HPNM equation of state

In most studies, in order to solve the nuclear equation of state at zero temperature ($T = 0$), the Thomas-Fermi model has been used. In this work, to insert the temperature effects in the EOS, we have employed the Seyler-Blanchard (SB) potential model which has been generalized by using the modified density-dependent terms [16]. This modified potential, which uses the Thomas-Fermi (TF) approximation, reproduced successfully the nuclear-matter potential. The modified SB potential of the present work gives a soft equation of state.

In general, the polarized nuclear matter is composed of the spin-up (spin-down) protons and spin-up (spin-down) neutrons. Thus,

$$A = N\uparrow + N\downarrow + P\uparrow + P\downarrow \tag{4}$$

is the total number of nucleons. In this relation, $N\uparrow$ ($N\downarrow$) and $P\uparrow$ ($P\downarrow$) are the numbers of spin-up (spin-down) neutrons and protons, respectively. The corresponding densities are $\rho_{n\uparrow}$, $\rho_{n\downarrow}$, $\rho_{p\uparrow}$, and $\rho_{p\downarrow}$. Therefore, in this formalism the total density of nuclear matter ρ is given by

$$\rho = \rho_n + \rho_p = \rho_{n\uparrow} + \rho_{n\downarrow} + \rho_{p\uparrow} + \rho_{p\downarrow}. \tag{5}$$

The useful parameters to analyze the HPNM equation of state in the framework of the SB model are defined in the following formalism: The neutron excess parameter

$$X = (\rho_n - \rho_p)/\rho, \tag{6}$$

the neutron spin-up excess parameter

$$\alpha_n = (\rho_{n\uparrow} - \rho_{n\downarrow})/\rho, \tag{7}$$

TABLE I. The radius (R_0) and diffuseness (a_0) parameters of projectile and target nuclei. For ^{40}Ar, these parameters were taken from the 2PF distribution [33] and, for ^{40}Ca, they were taken from the 3PF distribution, for which the parameter w was taken to be zero [34]. In this table, the value of the quadrupole (β_2) and hexadecapole (β_4) deformation parameters are shown. Values of these parameters are determined by an HFB calculation [35].

Nucleus	R_0 (fm)	a_0 (fm)	β_2	β_4
^{40}Ar	3.53	0.542	0.00	0.00
^{40}Ca	3.766	0.544	0.00	0.00

the proton spin-up excess parameter,

$$\alpha_p = (\rho_{p\uparrow} - \rho_{p\downarrow})/\rho, \tag{8}$$

and

$$Y = \alpha_n + \alpha_p, \tag{9}$$

$$Z = \alpha_n - \alpha_p, \tag{10}$$

are a measure of the asymmetric and polarization characteristics of the HPNM. In this model the energy per nucleon at temperature T and density ρ is defined as

$$E(\rho, T) = E_0(\rho, T = 0) + E_T(\rho, T), \tag{11}$$

where $E_0(\rho, T = 0)$ is the energy per nucleon at zero temperature and $E_T(\rho, T)$ is the temperature-dependent part of the energy per nucleon, which is given by [16]

$$E_T(\rho, T) = -\frac{T^2}{6}\left(\frac{2m^*}{\hbar^2}\right)\left(\frac{3\pi^2}{2}\right)^{1/3}\rho^{-2/3}, \tag{12}$$

where m^* is the nucleon effective mass and is given by

$$m^* = m\left[1 + \frac{m}{\hbar^2}\left(\frac{4a^3ck_f^3}{3\pi b^2}\right)\right]^{-1}, \tag{13}$$

where m is the nucleon mass and k_f is the Fermi momentum. By using the adjustable parameters from Ref. [16], the value of the nucleon effective mass is $m^*/m = 0.974$. We refer the reader to Ref. [17], where the detailed method of calculation is explained.

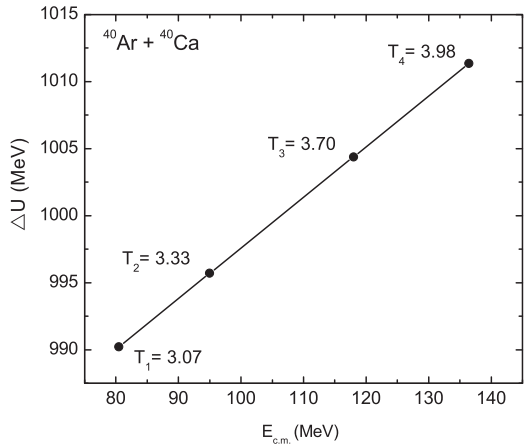

FIG. 2. Variations of energy due to complete overlap of two colliding nuclei in terms of the projectile nucleus energy. The temperature corresponding to each energy is also shown.

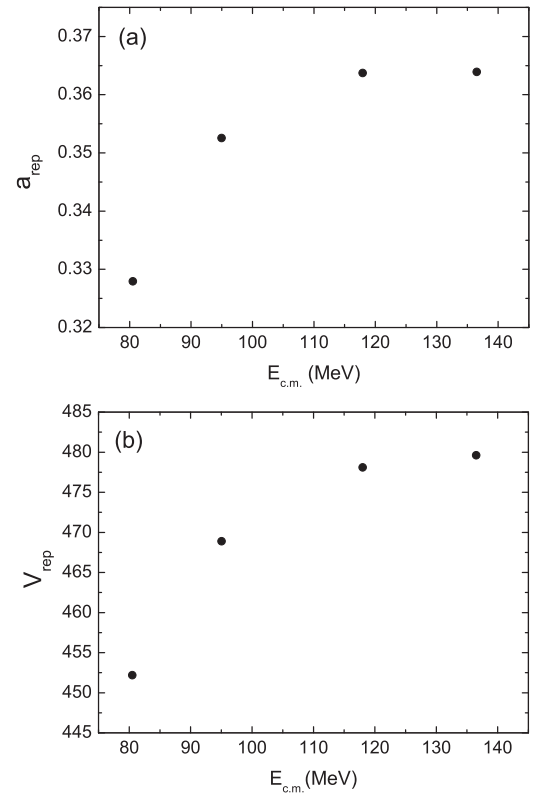

FIG. 3. Variations of parameters used in calculation of repulsive part of nuclear potential (a) a_{rep} and (b) V_{rep} in terms of the projectile-nucleus energy of the reaction ^{40}Ar + ^{40}Ca.

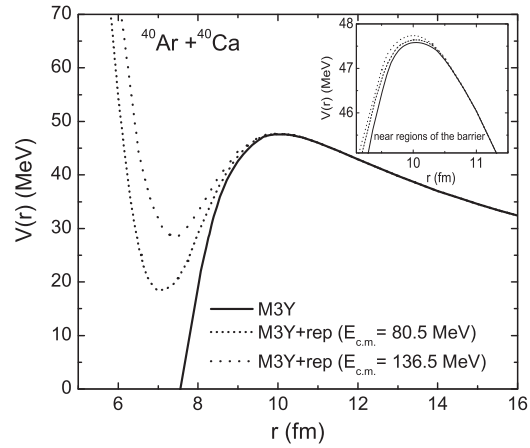

FIG. 4. Calculated total potentials for the system ^{40}Ar + ^{40}Ca. The solid curve is the M3Y potential. The short-dashed and dotted curves are based on the M3Y + repulsion potentials for $E_{c.m.} = 80.5$ MeV and $E_{c.m.} = 136.5$ MeV, respectively. The changes of interaction potential in regions near to the barrier are also shown.

TABLE II. Properties of the 2^+ and 3^- states in the projectile (^{40}Ar) and target (^{40}Ca) nucleus [21,22].

Nucleus	λ^π	E_x (MeV)	$B(E\lambda)(e^2b^\lambda)$	β_λ
^{40}Ca	2^+	3.904	0.0099	0.123
^{40}Ca	3^-	3.737	0.0204	0.432
^{40}Ar	2^+	1.460	0.0330	0.251
^{40}Ar	3^-	3.681	0.0087	0.314

III. ION-ION POTENTIAL

In this paper, to calculate internuclear potential, we have employed the DF model. The interaction between two ions in this model can be evaluated as the double-folding integral

$$V(\mathbf{r}) = \int d\mathbf{r}_1 \int d\mathbf{r}_2 \rho_1(\mathbf{r}_1) \upsilon(\mathbf{r}_{12}) \rho_2(\mathbf{r}_2), \tag{14}$$

where $\mathbf{r}_{12} = \mathbf{r} + \mathbf{r}_1 - \mathbf{r}_2$ and $\mathbf{r}$ is the distance between the centers of the two interacting nuclei. In our calculations the density distribution functions of the target and projectile nuclei are assumed to be of the form of the Fermi-Dirac distribution function

$$\rho_i(r) = \frac{\rho_0}{1 + \exp\left[(r - R_{0i})/a\right]}, \tag{15}$$

where $R_{0i} = r_{0i} A_i^{1/3}$. Equation (14) has been calculated by the simulation method we proposed earlier [18], using the M3Y-Reid interaction with a zero-range exchange part. The direct and exchange parts of this force are given by [19]

$$\upsilon_{\rm dir}(\mathbf{r}_{12}) = \upsilon_{00}(\mathbf{r}_{12}) + \frac{N_1 - Z_1}{A_1}\frac{N_2 - Z_2}{A_2}\upsilon_{01}(\mathbf{r}_{12}), \tag{16}$$

$$\upsilon_{\rm ex}(\mathbf{r}_{12}) = \left(\hat{J}_{00}(\mathbf{r}_{12}) + \frac{N_1 - Z_1}{A_1}\frac{N_2 - Z_2}{A_2}\hat{J}_{01}(\mathbf{r}_{12})\right)\delta(\mathbf{r}_{12}), \tag{17}$$

with the explicit form of the expressions for υ_{00}, υ_{01}, $\hat{J}_{00}$, and $\hat{J}_{01}$ given, for example, in Ref. [20]. The DF model, in comparison with the more realistic models of potential, is not able to reproduce the potential values in the interior regions. Modifying the effects of repulsive core has eliminated this problem. In the study of heavy-ion fusion reactions, the simulation of the effects of repulsive core on the calculation of the nuclear potential has been done by adding a zero-range interaction in the suggested form, $\upsilon_{\rm rep}(\mathbf{s}) = V_{\rm rep}\delta(\mathbf{s})$, to the NN interaction. In this form, the parameter $\mathbf{s}$ is the distance between the two interacting nucleons. Indeed, accounting

TABLE III. Parameters for WS potential determined by fitting to M3Y + repulsion potentials. The fitting has been done in the region of the fusion radii. The relative error of fitting the WS potential to the M3Y + repulsion potentials in each energy is less that 10^{-7}.

$E_{\rm c.m.}$ (MeV)	V_0	r_0	a
80.5	74.80	1.159	0.729
95	68.02	1.162	0.750
118	61.02	1.176	0.741
136.5	62.06	1.172	0.748

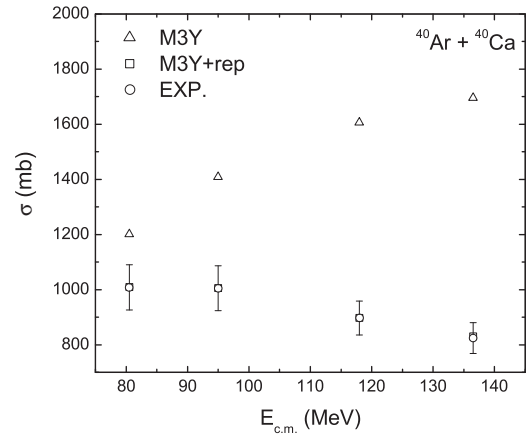

FIG. 5. Fusion cross sections resulting from M3Y and M3Y + repulsion potentials are compared to experimental data for ^{40}Ar + ^{40}Ca reaction [23].

for the effect of the nuclear-matter incompressibility in the calculation of the nucleus-nucleus potential in the double-folding model requires that a repulsive part, $V_{\rm rep}(\mathbf{r})$, be added to the attractive part, $V_{\rm atr}(\mathbf{r})$, such that

$$V_{NN}(\mathbf{r}) = V_{\rm atr}(\mathbf{r}) + V_{\rm rep}(\mathbf{r}). \tag{18}$$

The attractive part of the nuclear potential can be evaluated as the double-folding integral by Eq. (14). The repulsive part of the nuclear potential can be calculated using

$$V_{\rm rep}(\mathbf{r}) = \int d\mathbf{r}_1 \int d\mathbf{r}_2 \rho_1(\mathbf{r}_1) V_{\rm rep}\delta(\mathbf{r}_{12})\rho_2(\mathbf{r}_2). \tag{19}$$

In the calculation of this integral it is assumed that the diffuseness parameter for the density distribution of target and projectile nuclei is equal to $a_{\rm rep}$. In order to calculate the constants used in the simulation of the repulsive core (i.e., $a_{\rm rep}$ and $V_{\rm rep}$), the following relation has been used:

$$\Delta U = V_{NN}(0), \tag{20}$$

where $V_{NN}(0)$ is equal to the nucleus-nucleus potential evaluated at $r = 0$; that is, at the completely overlapping nuclei region. The values of the parameters $a_{\rm rep}$ and $V_{\rm rep}$ at each energy are chosen such that the fusion cross sections obtained from the M3Y + repulsion potential have the best agreement with the experimental cross section.

TABLE IV. In this table the theoretical cross sections $\sigma_{\rm theor}$ are compared with experimental cross section $\sigma_{\rm expt}$. The quantities $\pm\delta\sigma$ are the experimental errors for the cross section. The experimental cross-section data are taken from Ref. [23]. T is the temperature of the compound system for every energy in units of MeV.

$E_{\rm c.m.}$ (MeV)	T (MeV)	$\sigma_{\rm theor}$ (mb)	$\sigma_{\rm expt}$ (mb)	$\pm\delta\sigma$	χ [a]
80.5	3.074 02	1009.669 80	1008	82	0.165
95	3.333 17	1005.631 87	1005	81	0.062
118	3.706 99	897.095 20	897	61	0.010
136.5	3.981 42	831.075 69	824	56	0.858

[a] $\chi = 100[(\sigma_{\rm theor} - \sigma_{\rm expt.})/\sigma_{\rm expt}]$ is the percent error in the calculation of the cross section.

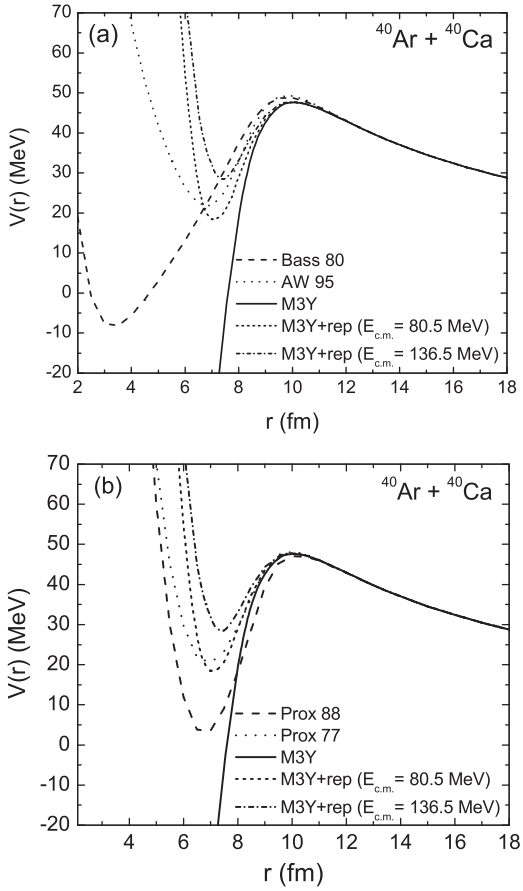

FIG. 6. Total interaction potential using different versions of proximity potential for (a) Bass 80 [25] and AW 95 [30] and (b) Prox 77 [24] and Prox 88 [25] are compared to M3Y and M3Y + repulsion (for energy $E_{\min} = 80.5$ MeV and $E_{\max} = 136.5$ MeV) potentials for ^{40}Ar + ^{40}Ca.

In this work we examined the ^{40}Ar + ^{40}Ca reaction. The three main reasons that we have chosen this reaction to investigate our proposed formalism are the following: (a) The projectile nucleus (^{40}Ar) is asymmetric, so the compound nucleus (^{80}Sr) produced in this reaction is asymmetric with respect to the number of the neutrons and protons. The radius, diffuseness, and deformation parameters of the interaction nuclei have been listed in Table I. (b) The target and projectile nuclei are spherical and also are in their ground state (see Table I). (c) The temperature of the compound nucleus in this reaction increases to above 3 MeV. The variation in the calculated values of ΔU in the range of the compound nucleus temperature (i.e., 3.07 to 3.98 MeV) are noticeable. In Fig. 2 the calculated variation of energy, ΔU [using Eq. (2)], for this reaction is plotted in terms of the projectile energy. When considering temperature (or energy) effects in modeling the repulsive core, the parameters used in the modeling (i.e. a_{rep} and V_{rep}) are dependent on the energy of the projectile nucleus. Changes in the parameters a_{rep} and V_{rep} in terms of projectile energy in the center-of-mass system $E_{\text{c.m.}}$ have been plotted in Fig. 3.

Nuclear matter incompressibility effects cause the appearance of shallow pockets in the inner part of the interaction potential. With increasing energy (or temperature) in the system, the effect of the repulsion force increases and leads to the reduction of the potential depth. The total interaction potential before and after applying nuclear-matter incompressibility effects have been shown in Fig. 4. The solid curve is based on the M3Y potential whereas the short-dashed and dotted curves are based on the M3Y + repulsion potential in $E = 80.5$ MeV (or $T = 3.07$ MeV) and $E = 136.5$ MeV (or $T = 3.98$ MeV), respectively. This figure shows that the effects of increasing ΔU on the inner part of the barrier and depth of the potential are considerable.

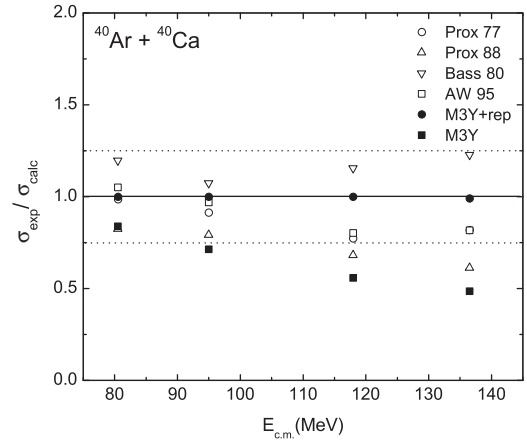

FIG. 7. Ratio of experimental [23] and calculated values of fusion cross section resulting from total interaction potential for Bass 80, AW 95, Prox 77, Prox 88, M3Y, and M3Y + repulsion potentials for ^{40}Ar + ^{40}Ca.

The theoretical cross sections in each energy have been derived using the CCFULL code. The CCFULL calculations are based on coupling low-lying 2^+ and 3^- states in both target and projectile nuclei with deformations parameters $\beta_\lambda^N = \beta_\lambda^C$. The structure input used to describe the excitation of the low-lying states 2^+ and 3^- in ^{40}Ar and ^{40}Ca is given in Table II [21,22]. To calculate the fusion cross section using the CCFULL code, a Woods-Saxon (WS) potential is fit to M3Y and M3Y + repulsion potentials in the region of the fusion-barrier radii. The parameters of the fit are given in Table III. The results of our calculations and their comparison with the experimental values are depicted in Fig. 5. This figure shows that considering the effects of the repulsive core at each energy significantly influences the fusion cross section and improves the agreement with experimental data [23]. The calculated values of the fusion cross sections are given in the Table IV.

In recent years many studies have been done using the proximity potential model. Modifications of the surface energy coefficient γ and nuclear radii R are two of the most important purposes of the investigation of this model and lead to different versions such as Prox 77 [24], Prox 88 [25], Prox 00 [26], and, recently, Prox 00DP [27]. The comparison between different versions of proximity potentials for symmetric and asymmetric colliding nuclei is given in Refs. [28–31]. In present work, in addition to using the DF model, we have calculated the total interaction potential by using of static models such as Bass 80 [25], AW 95 [32], and two versions of proximity potential (i.e., Prox 77 and Prox 88, see Fig. 6). In Fig. 7

the ratio of experimental and calculated values of the fusion cross section for different versions of proximity potential are plotted. This figure shows that our results for the fusion cross section are in good agreement with experimental data and with the results obtained from Prox. 77 and Prox. 88 potentials in energies $E_{\text{c.m.}} = 80.5$ MeV and $E_{\text{c.m.}} = 95$ MeV. The discrepancy between our results for fusion cross section and the results of Prox. 77 and Prox. 88 potentials in energies $E_{\text{c.m.}} = 118$ MeV and $E_{\text{c.m.}} = 136.5$ MeV could be due to the effect of temperature of the compound nucleus, which we have considered in these calculations.

IV. CONCLUSIONS

In this paper we have investigated the effects of the incompressibility of nuclear matter on the fusion cross sections of heavy ions by adding a zero-range force to the nucleonic interaction and employing Eq. (2). Our results involving the $^{40}\text{Ar} + ^{40}\text{Ca}$ reaction reveal that the variation of the energy due to the complete overlapping of the two nuclei is considerable for a given variation of the temperature of the compound nucleus (see Fig. 2). The simulation of the effects of the incompressibility of nuclear matter on the calculation of the nuclear potential has been accomplished by including an energy-dependent interaction instead of the commonly used energy-independent interaction [2]. This is justified by the variations of the parameters a_{rep} and V_{rep} with the energy of the projectile nucleus, which is shown in Fig. 3. An increase in the values of the parameters a_{rep} and V_{rep}, results from raising ΔU to the range of the temperature of the compound nucleus. Our overall conclusion is that the use of the HPNM state equation and the simulation of the incompressibility of nuclear matter by an energy-dependent force have enabled us to simulate the incompressibility effects of nuclear matter for the heavy-ion fusion reactions in such a manner that a good agreement between the theoretical and experimental values of the cross sections has been achieved (see Table IV). The simulation of a repulsive core using an energy dependent force could be due to the decrease in the roll of the mean-field theory in compound nuclei when the excited temperature of compound nucleus increases above 2 MeV.

Since our proposed formalism for the nuclear-potential calculation depends on the temperature of the compound nucleus, it could well be suited for simultaneously accounting for the effects of the precompound neutron evaporation, which affects the Q value of the reaction, the temperature of the nucleus, and the incompressibility effects of nuclear matter on the calculation of the nuclear potential.

[1] S. Misicu and H. Esbensen, Phys. Rev. Lett. **96**, 112701 (2006).
[2] S. Misicu and H. Esbensen, Phys. Rev. C **75**, 034606 (2007).
[3] E. Uegaki and Y. Abe, Prog. Theor. Phys. **90**, 615 (1993).
[4] C. L. Jiang *et al.*, Phys. Rev. Lett. **93**, 012701 (2004).
[5] C. L. Jiang *et al.*, Phys. Rev. C **71**, 044613 (2005).
[6] C. L. Jiang, B. B. Back, H. Esbensen, R. V. F. Janssens, and K. E. Rehm, Phys. Rev. C **73**, 014613 (2006).
[7] C. L. Jiang *et al.*, Phys. Rev. C **78**, 017601 (2008).
[8] H. Esbensen and C. L. Jiang, Phys. Rev. C **79**, 064619 (2009).
[9] C. L. Jiang, K. E. Rehm, B. B. Back, and R. V. F. Janssens, Phys. Rev. C **79**, 044601 (2009).
[10] O. N. Ghodsi and V. Zanganeh, Nucl. Phys. A **846**, 40 (2010).
[11] W. D. Myers and W. J. Swiatecki, Phys. Rev. C **57**, 3020 (1998).
[12] R. K. Puri *et al.*, Nucl. Phys. A **575**, 733 (1994).
[13] Y. K. Vermani, S. Goyal, and R. K. Puri, Phys. Rev. C **79**, 064613 (2009).
[14] Y. K. Vermani and R. K. Puri, Nucl. Phys. A **847**, 243 (2010).
[15] W. D. Myers and W. J. Swiatecki, Act. Phys. B **26**, 111 (1995).
[16] H. M. M. Mansour and Kh. A. Ramadan, Phys. Rev. C **57**, 1744 (1998).
[17] H. M. M. Mansour, M. Hammad, and M. Y. M. Hassan, Phys. Rev. C **56**, 1418 (1997).
[18] O. N. Ghodsi, M. Mahmoodi, and J. Ariai, Phys. Rev. C **75**, 034605 (2007).
[19] G. Bertsch, W. Borysowicz, H. McManus, and W. G. Love, Nucl. Phys. A **284**, 399 (1977).
[20] G. R. Satchler and W. G. Love, Phys. Rep. **55**, 183 (1979).
[21] S. Raman, C. W. Nestor JR., and P. Tikkanen, At. Data Nucl. Data Tables **78**, 1 (2001).
[22] R. H. Spear, At. Data Nucl. Data Tables **42**, 55 (1989).
[23] J. Carter, C. Brendel, A. Richter *et al.*, Z. Phys. A Atoms and Nuclei **313**, 57 (1983).
[24] J. Blocki, J. Randrup, W. J. Swiatecki, and C. F. Tsang, Ann. Phys. (NY) **105**, 427 (1977).
[25] W. Reisdorf, J. Phys. G **20**, 1297 (1994).
[26] W. D. Myers and W. J. Swiatecki, Phys. Rev. C **62**, 044610 (2000).
[27] G. Royer and R. Rousseau, Eur. Phys. J. A **42**, 541 (2009).
[28] I. Dutt and R. K. Puri, Phys. Rev. C **81**, 044615 (2010).
[29] I. Dutt and R. K. Puri, Phys. Rev. C **81**, 064609 (2010).
[30] I. Dutt and R. K. Puri, Phys. Rev. C **81**, 064608 (2010).
[31] I. Dutt and R. K. Puri, Phys. Rev. C **81**, 047601 (2010).
[32] A. Winther, Nucl. Phys. A **594**, 203 (1995).
[33] H. de Vries, C. W. deJager, and C. de Vries, At. Data Nucl. Data Tables **36**, 495 (1987).
[34] I. I. Gontchar, D. J. Hinde, M. Dasgupta, and J. O. Newton, Phys. Rev. C **69**, 024610 (2004).
[35] http://www-nds.iaea.org/RIPL-2/masses.html